Effect of Sodium Bromide on the Electrodeposition of Sn, Cu, Ag and Ni from a Deep Eutectic Solvent-Based Ionic Liquid

Hasan F Alesary[1,], Ahmed F Khudhair[1], Saad Y. Rfaish[1], Hani K Ismail[2]*

[1] Department of Chemistry, College of Science, University of Kerbala, Karbala, Iraq.
[2] Department of Chemistry, Faculty of Science and Health, Koya University, Koya, Kurdistan Region Iraq.
[*]E-mail: hasan.f@uokerbala.edu.iq

A number of studies into the influence of additives on the electrodeposition of metals from aqueous solution have been reported in the literature. However, very few have studied the influence of additives on metal electrodeposition in Deep Eutectic Solvents (DESs). This work will show, for the first time, the effect of sodium bromide on the electrodeposition of tin, copper, silver and nickel from a deep eutectic solvent (DES)-based ionic liquid consisting of a stoichiometric 1:2 mix of choline chloride and ethylene glycol (*Ethaline 200*). It is shown that in the presence of sodium bromide, bright and smooth Cu and Ni deposits were formed. Cyclic voltammetry and chronocoulometry have been used to examine the electrochemical properties of the plating liquids in both the absence and presence of sodium bromide. It was found that the redox peak currents of the Sn and Ag electrolytes get smaller when sodium bromide is added to the electrolyte solution. The resultant surface morphologies, topography and roughness of Sn, Cu, Ag and Ni were investigated by scanning electron microscopy (SEM/ EDXS) and 3D optical microscopy (3D). The current efficiency of metal deposits was found to increase when the deposition was achieved from an electrolyte that contained sodium bromide.

1. INTRODUCTION

Electroplating plays a significant role in many large–scale manufacturing applications such as the production of corrosion-resistant and decorative coatings.[1, 2] Electroplating allows for the coating of objects such as electronics, optical sensors and aerospace components with metals.[2] Various metals such as Ni, Cu, Co, Zn, Sn, Cr, Ag, Al, etc., have all been used in the electroplating of objects, where their use serves various purposes such as decoration, corrosion resistance, hardness and increased thermal stability of the surface.[3] Plating with Cr, Ni, or Co gives a hard coating, while Zn

and Cd can provide coatings with anticorrosion properties, and Au and Ag are employed for improved cosmetic appearance.[4] In recent years, the electrodeposition of Sn has received considerable attention due to its non-toxicity, high resistance to corrosion, good ductility and its potential for use in electrochemical applications such as electronics and batteries.[5-9] Sn and its alloy coatings have been used in numerous industrial applications such as the automobile industry,[10] microelectronics,[11] aeronautics,[12] and the food industry.[13] Sn and its alloys have been widely used for imparting corrosion resistance to active metal substrates in aggressively corrosive environments. In addition, Sn is non-toxic compared to metals such cadmium (toxic) and nickel (allergenic). Sn deposits can be offer high corrosion protection for steel, good frictional properties and ductility after plating, and good solderability.[14] In the past, tin electrodeposition was achieved in aqueous solution. However, there are some disadvantages to using aqueous media in this manner such as excessive hydrogen evolution, low current efficiency, a narrow positional window and toxicity (cyanide).[15] Furthermore, the electrodeposition of some metals, for example W, Al and Ti, cannot occur in aqueous solution because of their sensitivity to water and the formation of a passivation layer (oxide or hydroxide layers), which makes coating with such metals difficult,[1, 15, 16] whilst metals such as Zn and Cr are poorly electrodeposited from aqueous electrolytes. Recently, metal electrodeposition has been achieved from ionic liquid media because these liquids have excellent physical properties compared to aqueous solutions, such as their high solubility for metal salts, a wide potential window and high current efficiency in the electroplating of metals.[15, 17-19]

Copper electrodeposition is fundamental to a diverse range large-scale industrial processes, especially in the field of electronics in the production of printed circuit boards, solidifying steel for building parts, and the production of electrotypes in the printing industry.[20, 21] Copper can be electroplated and deposited with different metals in a straightforward manner, and thus is especially valuable as a precoating for delicate soldering work or for alloys of zinc, such as those utilized extensively by the automotive industry. The copper deposit forms a 'defensive' layer on the substrate metal, enabling further coatings to be incorporated.[22]

Silver has been used widely for coatings due to its excellent physicochemical and antibacterial properties and good resistance to corrosion, high bulk conductivity and, of course, for decorative purposes.[23-25] Electrodeposition of Ag is used in the automotive, aerospace and microelectronics fields, amongst others. The work of Hussey and co-workers included a discussion of chloroaluminate salts, which are considered to be water sensitive.[26, 27] Hussey investigated silver electrodeposition on an assortment of cathodes in a 2:1 aluminium chloride:1-methyl-3-ethylimidazolium chloride ionic fluid at 40ºC, which resulted in the formation of a black Ag coating. Recently, Abbott and co-workers studied the electrodeposition of Ag in an ethylene glycol/choline chloride-based deep eutectic solvent. However, the properties of Ag deposits still need to optimized in such media.[28]

The electrodeposition of nickel and it alloys is vital to the functionalization of surfaces in terms of resistance to corrosion, magnetic applications and electrocatalysis.[29-36] The electrodeposition of Ni and Ni alloys has been studied in chloroaluminate ionic liquids (ILs), which were considered the pioneer generation of ILs in general.[37-40] The hygroscopic nature of chloroaluminate ILs has limited their use, however, since they need to be prepared under an inert environment. Moisture- and

air-stable ILs, which are regarded as the second class of ILs, have since gained considerable interest in numerous fields.

In this work, a new class of ionic liquids, called deep eutectic solvents (DESs), have been used in the electrodeposition of various metals. A DES can be synthesised by mixing two types of solid compounds that have high melting points, which leads to the production a liquid with a lower melting point than either of its individual compounds. The first type of DES is prepared by mixing choline chloride (ChCl) with urea (1:2).[41] DES has excellent properties such as a wide potential window, non-flammability, is inexpensive, non-toxic and has a high current efficiency for metal deposition.[41, 42] DESs can be used in various important industrial fields such as electropolishing,[43, 44] electroplating,[19, 45, 46] metal oxide processing[47] and polymer synthesis.[48-51] This type of liquid has solved some of the more pressing problems associated with the electrodeposition of metals from aqueous and non-aqueous solutions, and from which the electrodeposition of Zn,[17] Ni,[52] Cu,[53] Cr,[54] Ag, Sn and Co has been achieved. However, relatively little research has actually examined the electrodeposition of metals from DESs, or indeed the effects of additives on the same.

In the electroplating of metals from aqueous solution, additives have been used to optimize the physical and mechanical properties of the resultant coatings.[11, 55, 56] The additives work as brightening, levelling or grain-refining agents, where such media have been observed to affect the brightness of the coating, the grain size of metal and the throwing power; indeed, some additives can affect the anodic depolarisation and current efficiency.[57, 58] The additives appear to work in either of two ways: in the first, they can be adsorbed on the electrode surface, preventing the metal from being deposited on the sites occupied by the organic molecules. Levelling molecules will be adsorbed on the active sites or high points of the electrode surface, where at the latter the thickness of the diffusion layer is lower than in the recesses, and thus organic molecules will be transported faster; consequently, adsorption of organic molecules in the recesses will be reduced, and metal deposition tends to favour the recesses in the electrode surface. In the second, the additives can act as complexing agents, which can react with the metal ions in solution and make them more difficult to reduce.[17, 57-59]

There have been relatively few studies into the effects of additives on metal electrodeposition in DESs, despite the potential importance of these processes and the ubiquitous use of brighteners and levellers in aqueous solutions. Electrodeposition of metals from ionic liquids has previously been studied, but the deposits so produced were dull and showed poor adhesion. Our previous work (on the effects of boric acid, nicotinic acid and *p*-benzoquinone on the electrodeposition of Zn) was achieved from Ethaline 200.[59] The novelty of this work lies in the use of sodium bromide as an additive for the electrodeposition of Sn, Cu, Ag and Ni from Ethaline 200 (a 1:2 ChCl:EG-based liquid). NaBr was chosen as the additive as it is in common use as a brightener in the electroplating of metals from aqueous solutions. The physical and mechanical properties of metal deposited with NaBr as an additive have been found to be improved compared to the corresponding systems without NaBr, where bright Cu and Ni coatings were obtained for the first time as a result of adding NaBr to the plating bath. Cyclic voltammetry has been used to study the reduction mechanism of Sn, Cu, Ag and Ni in Ethaline 200 in both the presence and absence of NaBr; in addition, the effects of NaBr on the deposit morphology and roughness of the metal deposit have also been investigated.

2. EXPERIMENTAL

Choline chloride [$HOC_2H_4N(CH_3)_3Cl$] (ChCl) (Aldrich 99 %) and ethylene glycol (EG) (Aldrich +99%), were used as received. The two components were mixed under stirring (in a 1:2 molar ratio of ChCl: hydrogen-bond donor) at 70°C until a homogeneous, colourless liquid had formed.

The metal halide salts $SnCl_2$ (Aldrich 98%), $CuCl_2.2H_2O$ (Aldrich $\geq$ 98 %), AgCl (Aldrich 99%), and $NiCl_2.6H_2O$ (Aldrich 98%) were used; the concentration of each metals salt solution was made up to 0.05 mol/L. Sodium bromide, NaBr (Aldrich 99%), was used as received.

Cyclic voltammetry and chronocoulometry were performed using a FAB2 µAutolab type III potentiostat/galvanostat controlled via the GPES software suite. Three electrodes were used in this method: a platinum electrode (0.5 mm^2 area) as a working electrode; a platinum flag counter-electrode (made in-house) and an Ag/AgCl reference electrode. The working electrode was polished for 1 hour using 0.3 µm alumina paste, and then washed with distilled water and acetone. The polishing process was repeated prior to each experiment.

Cyclic voltammetry of $SnCl_2$, $CuCl_2.2H_2O$, AgCl and $NiCl_2.6H_2O$ was performed within a particular potential window for each salt, which for Sn was -0.3 to -0.9 V, for Cu was +1 to -1 V, for Ag was +0.4 to -0.3 V and for Ni was +0.5 to -1 V. All experiments were run at room temperature and at scan rates of 10 mV/s, and with various different concentrations of NaBr. The sweep potential was started from zero and pursued in the negative direction, after which it was reversed towards the positive potential.

Electrodeposition of Sn, Ag and Ni was achieved on a Cu substrate (copper, 50 mm $\times$ 42 mm $\times$ 1 mm). All experiments were performed using an Ethaline 200 medium containing 0.05 M $SnCl_2$, AgCl and $NiCl_2.6H_2O$. Bulk electrolysis was carried out with and without the addition of NaBr. The cathode substrate was, firstly, etched in ammonium persulfate solution, $(NH_4)_2S_2O_8$, washed with water and then dried under nitrogen. The anode was a Ti mesh, 40 mm $\times$ 50 mm, which had an iridium oxide coating. The electrodepositions were performed at room temperature and at a current density of 10 mA cm^{-2} for 30 mins.

The surface morphology was characterized using scanning electron microscopy (SEM), whilst the elemental analysis of the deposit compositions was carried out via energy dispersive X-ray spectroscopy (EDX) using a Phillips XL30 ESEM instrument with an accelerating voltage of between 15 and 20 keV, giving an average beam current of *ca.* 120 µA SEM/EDX. These techniques are essential to studying changes in surface topography and composition.

The Zeta-20 optical 3D-microscope technique was employed to provide a 3D image of the film and to measure the roughness of the coating. The Zeta-20 enables imaging of surfaces with very low reflectivity and very high roughness.

3. RESULTS AND DISCUSSION

3.1. Cyclic voltammetry studies

Cyclic voltammetry was employed to study the electrochemical behaviour of Sn, Cu, Ag, and Ni in Ethaline 200. Fig. 1 shows separate cyclic voltammograms for 0.05 M solutions of $SnCl_2$,
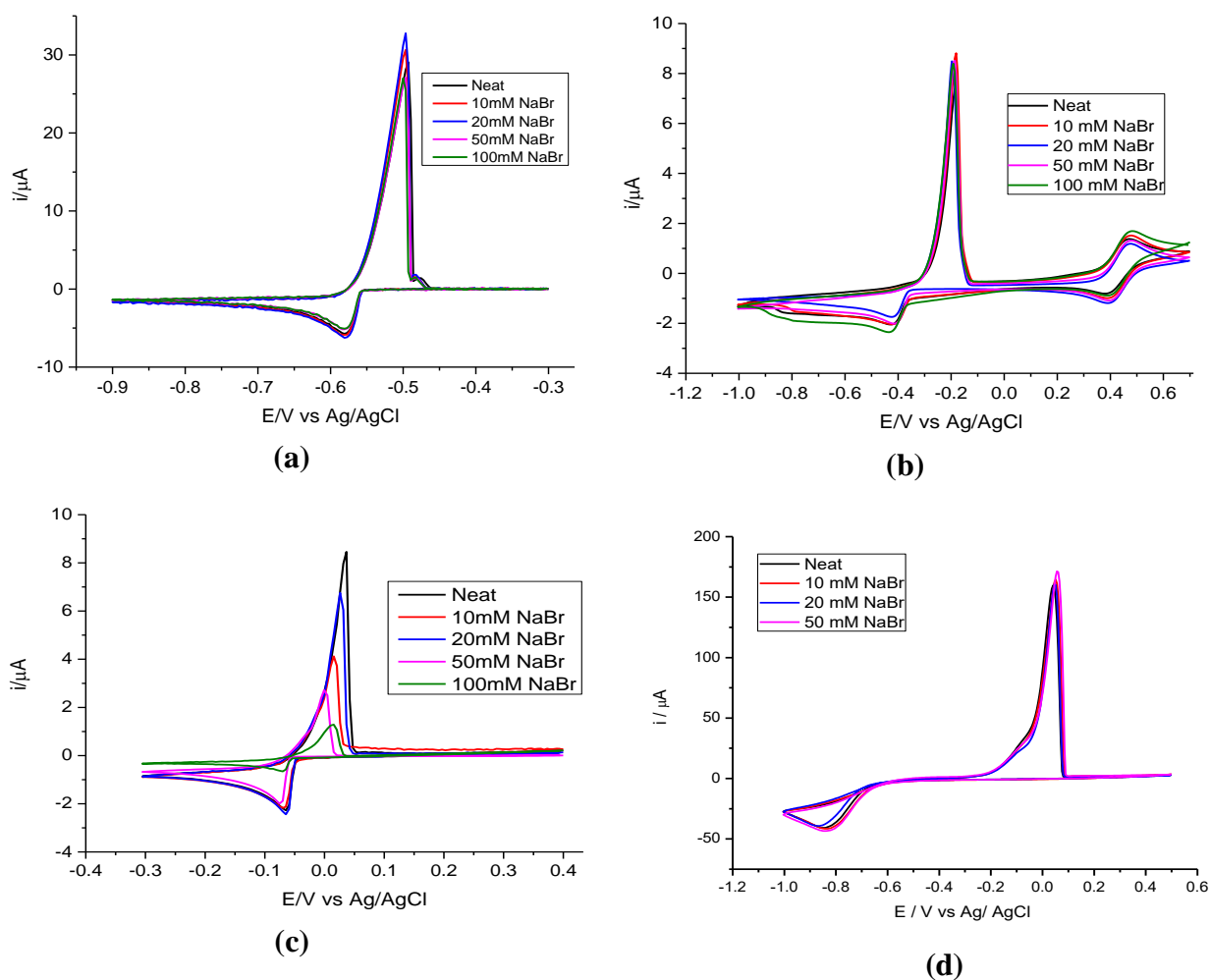
CuCl$_2$.2H$_2$O, AgCl, and NiCl$_2$.6H$_2$O in Ethaline 200. The voltammograms were performed at scan rates of 10 mVs^{-1} at room temperature using three electrodes, namely a 0.5 mm Pt disc electrode, a Pt flag counter-electrode and an Ag/AgCl reference electrode. The sweep potential was started at zero and pursued in the negative direction, and was then reversed in the direction of the positive potential. It is clear from Fig. 1 that the anodic stripping peak for Sn was at -0.53 V while the cathodic reduction peak can be seen at -0.57 V, similar to other studies performed using ionic liquids.[60, 61]. In Fig. 1, it can be seen from the cathodic scan that Ag species reduced at about -0.06 V while the dissolution peak current appeared at a more positive potential of +0.015 V. In other studies, underpotential (UPD) was detected when examining the effects of 0.1 M AgCl$_2$ in a deep eutectic solvent on a gold electrode.[28] However, this phenomenon was not observed in this work. In Fig. 1, voltammograms of copper showed two stripping peaks and two reducing peaks, where the first stripping peak indicated the conversion of Cu^0 to Cu^{1+}, which occurred at about -0.25 V, while the second stripping peak, which was observed at +0.45 V, corresponded to the conversion of Cu$^+$ to Cu^{2+}. The first reducing peak for Cu was shown at +0.51 V which corresponded to the reduction of Cu^{2+} to Cu$^+$, whilst the second reducing peak at -0.33 V and indicated the reduction of Cu$^+$ to Cu^0, in the process of which metallic copper was deposited on the electrode surface. The above was identical to previous work reported in the literature,[51, 53, 62] where the Abbott group studied the electrolytic deposition of Cu coatings in ionic liquids. They found that Cu species have two stripping and reduction potentials. Ni species in 1:2 ChCl:EG-based liquid started to reduce at -0.7 V, comparable with our previous work which described the electrodeposition of Zn-Ni alloy from Ethaline 200-based ionic liquids.[19] Recently, the Ryder group investigated the electrochemical properties of Ni species in eutectic liquids[63, 64] in which it was found that Ni species started to reduce at about -0.65 V, which is extremely close to the redox potential of the Ni complexes studied in this work. Fig. 1 shows that each metal was reduced at a different potential, where notably the Sn species started to reduce at -0.57 V and the Ag species at -0.06 V. A comparison between the voltammograms of these metals (Fig. 1) shows that Ni species need more energy to be deposited compared to that required to reduce the Ag, Sn and Cu species.
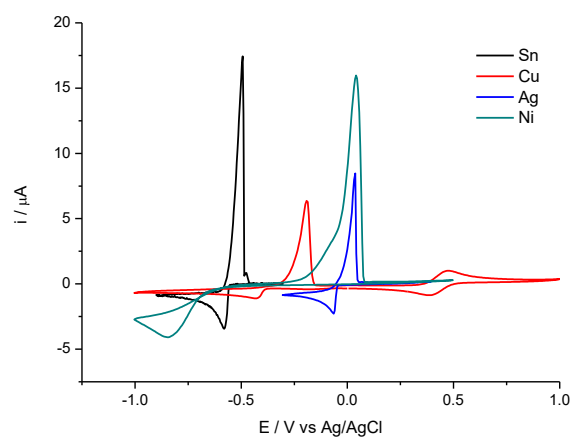
Figure 1. Cyclic voltammograms of 0.05 M SnCl$_2$, CuCl$_2$.2H$_2$O, AgCl and NiCl$_2$.6H$_2$O in Ethaline 200 using a 1 mm diameter Pt disc vs. Ag/AgCl reference electrode at a scan rate of 10 mV s^{-1} and at room temperature.

3.2. *Effect of sodium bromide on the voltammetric behaviour of metals*

Electrodeposition of Sn, Cu, Ag and Ni in a 1:2 mix of a choline chloride and ethylene glycol-based ionic liquid (Ethaline 200) was achieved at room temperature on a copper substrate. The deposition was performed in both the absence and presence of sodium bromide, with the latter at a concentration of 0.05 M. Therefore, it was considered interesting to study the cyclic voltammograms of these metals in Ethaline 200 under otherwise identical conditions. Fig. 2 demonstrates the cyclic voltammograms of 0.05 M $SnCl_2$, $CuCl_2.2H_2O$, $AgCl$, and $NiCl_2.6H_2O$ in Ethaline 200 with and without the sodium bromide additive.

Figure 2. Cyclic voltammograms of **a)** 0.05 M $SnCl_2$, **b)** 0.05 M $CuCl_2.2H_2O$, **c)** 0.05 M $AgCl$, and **d)** 0.05 M $NiCl_2.6H_2O$. All experiments were performed in Ethaline 200 with and without the addition of NaBr. The experiments were run at a potential scan rate of 10 mV s^{-1} and at room temperature using a Pt disc electrode vs. an Ag/AgCl reference electrode.

The voltammograms were run at room temperature at a scan rate of 10 mVs^{-1} using three electrodes, a 0.5 mm Pt disc as a working electrode, a Pt flag as a counter-electrode and an Ag/AgCl reference electrode. In Fig. 2 (a), reduction of tin (II) occurred at −0.581 V, while the maximum oxidation current peak for tin was observed at −0.493 V, which was essentially identical to the values

found in other studies in the literature.[60, 65] Different concentrations of sodium bromide were found to leave the general features of the CV unchanged, as shown in Fig. 2 (a). Therefore, it can be said that sodium bromide does not have any observable effect on the cyclic voltammograms of tin chloride in Ethaline 200.

Fig.2 (b) shows the voltammograms of 0.05 M $CuCl_2.2H_2O$ in Ethaline 200 in both the absence and presence of sodium bromide at concentrations of 10, 20, 50, and 100 mM. Obviously, there are two clear reduction processes: firstly, the reversible Cu (II)/Cu (I) couple at +0.380 V, and secondly the reduction of Cu (I) to Cu (0) at −0.465 V.[46, 53] In metallic copper, the latter process results in deposition on the anodic scan with a stripping response. Increases in the oxidation-reduction current peaks of Cu species were observed when the process was recorded using electrolytes containing NaBr. The addition of NaBr to the Cu electrolytes could help to prevents a passivation layer of copper oxide from forming on the electrode surface.[19, 66] In addition to surface passivation, NaBr may have an additional benefit in Cu electrodeposition by acting as a surfactant to enhance conformal Cu growth.[17, 66, 67]. In aqueous solutions, sodium bromide and/or sodium chloride is introduced to the plating baths to improve the conductivity and reduce the thicknesses of the passivation layers that form on the electrode surface. [68, 69] Thus, one of reasons for the increase in current intensity of Cu in Ethaline 200 in the presence of NaBr could be due to the subsequent minimization of the effects of the passivation layer.

Fig.2 (c) shows cyclic voltammograms of AgCl in Ethaline 200 in the absence of NaBr, where the reduction of Ag can be observed in Ethaline 200 at E = -1.20 V and where the oxidation peak of Ag occurred at E = -0.95 V, in agreement with other work by Abbott and co-workers.[28] There were slight decreases in the reduction current peaks for Ag when sodium bromide was added to the plating bath at concentrations of 10, 20, and 50 mM; the largest concentration of sodium bromide (100 mM) was found to block the surface of the electrode, which meant that less metal was deposited and thus that the stripping peak was smaller.[17, 19, 28, 59, 70]

As explained earlier, additives can be adsorbed onto the electrode surface and thus metal deposition cannot take place at the sites occupied by organic molecules. Molecules or additive ions will be adsorbed at the active sites or on the high points of the electrode surface, where the thickness of the diffusion layer is less than in the recesses; thus, molecules/ions will be transported faster.[57, 58, 71] Consequently, adsorption of additives molecules within the recesses will be considerably reduced and thus the metals will tend to deposit in the recesses in the electrode surface.

Here, in the voltammograms of Ag, there is a suggestion that NaBr is absorbed on the surface of the electrode and impedes the deposition of Ag in such regions. This was investigated in the electrodeposition of Sn in the presence of NaBr, where the Br⁻ anion was observed in the coating; the coating was examined using SEM/ EDX, as will be discussed in the surface analysis section. The presence of Br⁻ anions in the coating was indicated by the adsorption of NaBr on the electrode surface and thus its incorporation into the composition of the deposits. The adsorption of NaBr onto the electrode surface impeded the growth of Ag nuclei and thus decreased the Ag reduction and oxidation current peaks, as can be seen in Fig. 2 (c).

In Fig. 2 (d), a slight change can be seen in the voltammograms of Ni when sodium bromide was added to the plating bath; however, a significant change to the morphology of the resultant Ni

deposits (as demonstrated in the SEM image) was also observed. Recently, Ryder and co-workers investigated the effects of nicotinic acid, boric acid and methylnicotinate on the electrodeposition of Ni from eutectic solvents, where they found that these additives can increase the growth rate of the deposition.[64, 72] Thus, a more in-depth study needs to be performed to investigate the mechanism of electrodeposition of Ni and other metals from eutectic solvents. This might be achieved by examining the nucleation and the mechanism of metal growth through the use of chronoamperometry and atomic force microscopy (AFM).

3.3. Chronocoulometry

Fig. 3 shows the results of the chronocoulometry experiment conducted for all metals without additives. The results were obtained using 0.05 M solutions of $SnCl_2$, AgCl, $CuCl_2.2H_2O$ and $NiCl_2.6H_2O$ in a 1:2 ChCl:EG-based liquid. A Pt disc electrode, Pt mesh counter-electrode and Ag/AgCl reference electrode were used in this experiment. The results were measured using the reduction potential of each metal, which is characteristic to each element (Sn = - 0.6 V, Cu = -0.33 V, Ag = -0.059 V, Ni = -0.75 V). It is clear from Fig. 3 that charge increases with time. From this method, the plots obtained can be interpreted in terms of the concentration gradients in the solution immediately adjacent to the electrode surface. The chronocoulometry of 0.01 M $CuCl_2.2H_2O$ in Ethaline 200 was studied by Abbott [53] through the use of a Pt disc electrode, where it was found that metal growth was diffusion controlled. Ryder and Barron studied the chronocoulometry of Ni and Zn complexes in a choline chloride-based liquid, from which they suggested that the depositions of Ni and Zn were not diffusion controlled.[17, 63, 73]

In the current study, however, Fig. 3 demonstrates that the plots of charge vs. $t^{1/2}$ for the metals considered are non-linear, signifying that the processes are not controlled by diffusion.
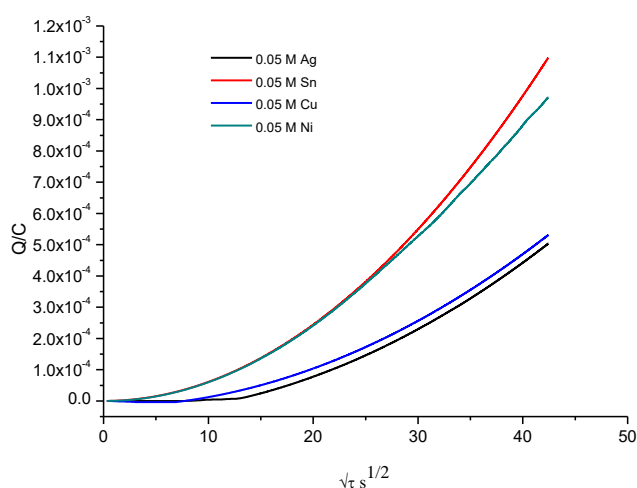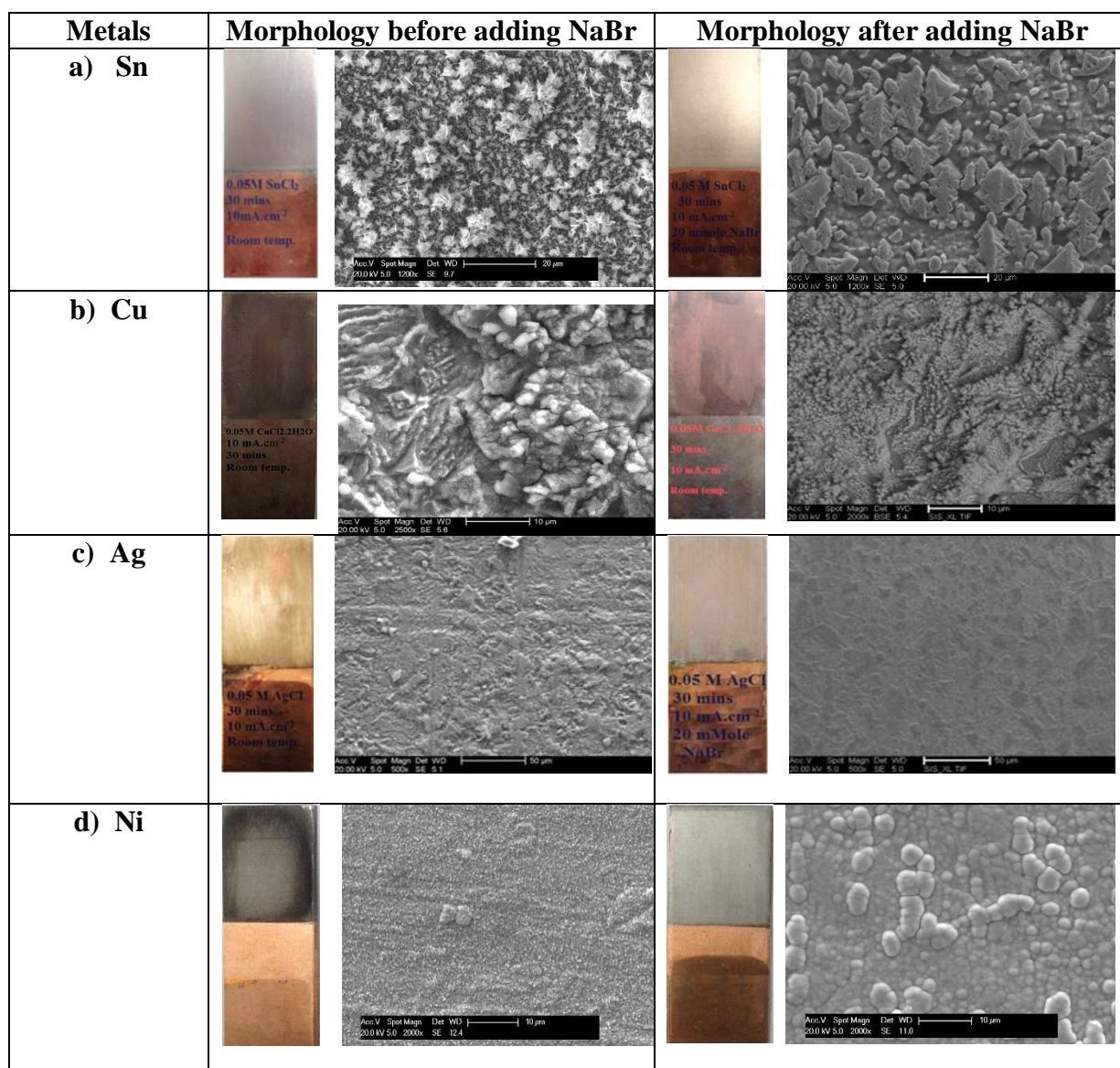

Figure 3. Chronocoulometry of 0.05 M $SnCl_2$, $CuCl_2.2H_2O$, AgCl and $NiCl_2.6H_2O$ in Ethaline 200 using a Pt disc (1 mm diameter) as the working electrode, a Pt flag counter-electrode and Ag/AgCl as the reference. All experiments were run for 1800 s.

3.4. SEM characterizations of the metal coating

In this work, SEM was used to study the effects of NaBr on metal electrodeposition from an Ethaline 200 base liquid. Fig. 4 shows the SEM and optical images of electroplating with Sn, Cu, Ag and Ni from Ethaline 200 both with and without NaBr at room temperature for 30 mins on a copper substrate using a current density of 10 mA cm^{-2}. Fig. 5 shows SEM images for the electrodeposition of (**a**) 0.05 M SnCl$_2$, (**b**) 0.05 M CuCl$_2$.2H$_2$O, (**c**) 0.05 M AgCl and (**d**) 0.05 M NiCl$_2$.6H2O in a 1:2 ChCl:EG-based liquid in both the presence and absence of NaBr.

Metals	Morphology before adding NaBr	Morphology after adding NaBr
a) Sn		
b) Cu		
c) Ag		
d) Ni		

Figure 4. SEM images for the electrodeposition of (**a**) 0.05 M SnCl$_2$ (**b**) 0.05 M CuCl$_2$.2H$_2$O, (**c**) 0.05 M AgCl and (**d**) **0**.05 M NiCl$_2$.6H$_2$O from Ethaline 200 in both the absence and presence of 0.02 M NaBr. All experiments were carried out at a current density of 10 mA.cm^{-2} for 30 mins. at room temperature.

A significant change can be seen in the morphology of the Sn deposit when the deposition was achieved from a bath containing sodium bromide, as is apparent from Fig. 4 (a). As discussed in the voltammetry section (Fig. 2), the NaBr seems to be preferentially adsorbed on the active points of the electrode surface. Adsorption of the additives at such active sites likely results in an increase in the current density and thus leads to an increased rate of Sn deposition. Otherwise, NaBr could be incorporated with the Sn deposition, which could also lead to an increase in Sn deposition rate; this was investigated using the EDX technique, as shown in Fig. 5. Here, Br$^-$ anions can be observed in the EDX data, which corresponds to the incorporation of NaBr into the Sn deposition. The current efficiency of the Sn deposit was about 90% before adding NaBr to the Sn electrolyte, but increased to 97.2% when NaBr was introduced into the plating bath. This increase in efficiency could correspond to the increase in the rate of Sn deposition due to adsorption of NaBr species on the cathode. Some additives can increase the polarization of the cathode.[57, 58, 74, 75] The adsorption of additives on the electrode surface can change the cathode potential, thus resulting in an increase in current density and the corresponding increase in current efficiency. However, there are some additives that can decrease cathodic polarization, such as pyridine derivatives.[76]

Fig. 4 (b) shows SEM images of Cu deposits on mild steal. It is clear from Fig. 4 (b) that the grain size of the Cu became smaller when the deposition was carried out in the presence of NaBr, and further that a bright Cu film formed when NaBr was added to the plating bath. Here, NaBr species could reduce the specific adsorption of chloride on the cathode surface. $[CuCl_4]^{2-}$ species were formed when $CuCl_2.2H_2O$ was dissolved in choline chloride-based liquid where this was proved by Jennifer.[77] A mixture of choline chloride and ethylene glycol (Ethaline 200) contains high concentrations of chloride, where the chloride ions tend to produce a black,[78] friable film due to their presence in the electrolyte increasing the number of nuclei at the surface of the electrode.[79, 80] High concentrations of Cl$^-$ ions could reduce the effectiveness and mobility of Cu species. NaBr may work in such a way as to reduce the specific adsorption of free chloride ions on the electrode surface and promote the process of Cu reduction, where the concentration of $[CuCl_4]^{2-}$ will be increased at the electrode surface as the activity and mobility of the chloride ions is decreased. Thus, NaBr can control the rate of nucleation and rate of increase of the growth of these nuclei, producing a bright Cu deposit as a result of adding NaBr to the plating liquid. The efficiency of Cu coating in Ethaline 200 is about 88%, but was found to increase to 95.7 % when the deposition was achieved from a medium containing NaBr. These values were calculated using the faraday law and from the weight of the sample before and after coating.
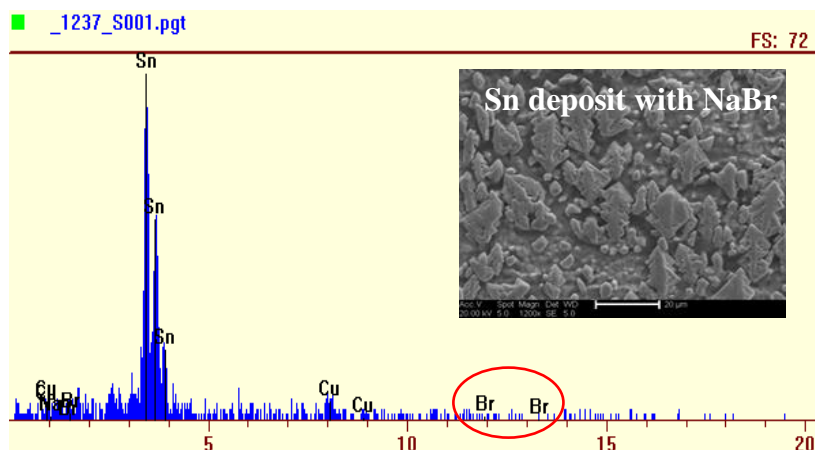
Figure 5. SEM and EDX for the electrodeposition of 0.05 M $SnCl_2$ in Ethaline 200 on a copper substrate in the presence of 0.02 M NaBr. All experiments were carried out at a current density of 3.75 mA cm^{-2} for 30 mins. at room temperature.

No significant change was observed in the Ag deposit morphology; however, it can be seen that the coating became increasingly homogenous when NaBr was used, as is clear from Fig. 5 (c). Here, NaBr increased the conductivity of the plating liquid by 0.32 mS cm^{-1}, thus increasing the rate of Ag deposition and, therefore, the current efficiency of the coating.
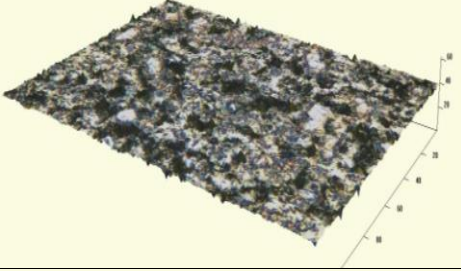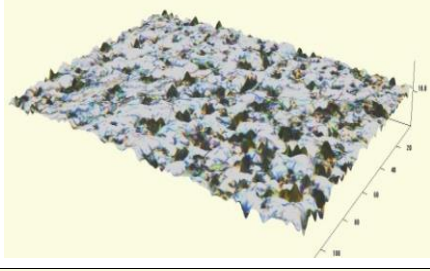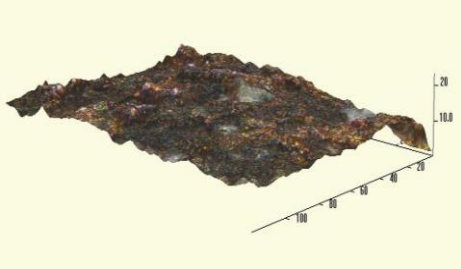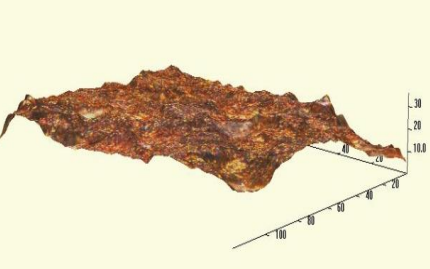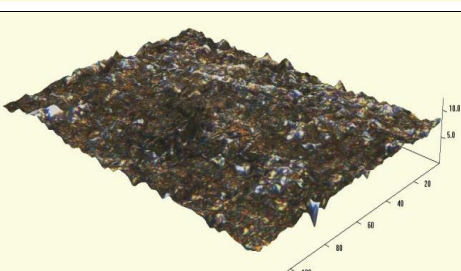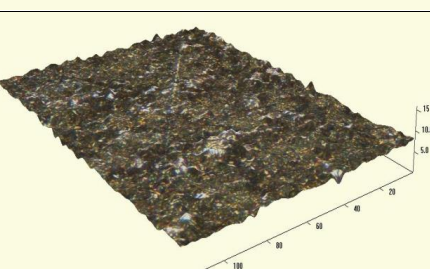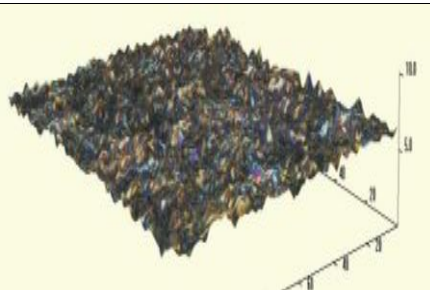
A significant change occurred in the Ni deposit morphology when the deposition was achieved from a system containing NaBr as an additive; a uniform, homogenous and bright Ni deposit was obtained in this latter instance. Here, NaBr helped to increase the conductivity and cohesion of the Ni coating. The current efficiency of the Ni deposit was between 89-90%, but increased to 98-99% when the deposition was achieved from the liquid medium containing NaBr. Therefore, it can be suggested that sodium bromide is a very effective brightener, producing highly uniform and smooth Ni deposits from an Ethaline 200-based eutectic solvent.

3.5. Surface Roughness

3D microscopy is one of the analytical methods utilized in this study. This method offers data about surface properties, for example, surface profile and roughness, but can additionally be applied to determine the thicknesses of surface coatings. In the current study, the Zeta-20 optical 3D- microscope has been utilized to examine the surface roughness studies of the metals used, and furthermore to give an indication of the 3D imagery of each coating. Fig. 6 shows the 3D microscopic images of electroplating with Sn, Cu, Ag and Ni from Ethaline 200 in both the absence and presence of 0.02 M NaBr. The processes were performed at room temperature for 30 mins. on a copper substrate at a current density of 10 mA cm^{-2}.

Fig. 6 shows the extensive change in the roughness of the metal deposits that can be achieved from liquid media containing NaBr, as is also clear from Table 1. Table 1 indicates the average surface roughness of metals coated. In this table, it can be seen that the roughness of the silver and nickel

coating increased as a result of using a 0.02 M NaBr concentration in the plating bath, while the roughness of the copper deposit significantly decreased when NaBr was used. The information reported in Table 1 can be characterized as follows: Rpv is the maximum peak to valley difference, Ra is the mean roughness, Rpv is the largest top to valley distinction, Rp is the maximum peak height, Rv is the maximum valley depth and average of (Rp – Rv) from five sections (Rz).

Metals	3D imaging of coating before addition of NaBr	3D imaging of coating after addition of NaBr
a) Sn		
b) Cu		
c) Ag		
d) Ni		

Figure 6. 3D microscopy images of **(a)** 0.05 M $SnCl_2$ **(b)** 0.05 M $CuCl_2.2H_2O$, **(c)** 0.05 M AgCl and **(d)** 0.05 M $NiCl_2.6H_2O$ depositions from Ethaline 200 in both the absence and presence of 0.02 M NaBr. All experiments were carried out at a current density of 10 mA cm^{-2} for 30 mins at room temperature.

Table 1. Average surface roughnesses for copper substrates plated with various metals

Metal	Ra / µm	Rpv/ µm	Rp/ µm	Rv/ µm	Rz/ µm
Sn	0.4095	6.951	4.542	2.410	5.856
Sn with 20 mM NaBr	0.6174	8.078	4.591	3.487	7.189
Cu	1.643	9.369	4.828	4.541	4.887
Cu with 20 mM NaBr	1.184	7.123	3.894	3.229	3.864
Ag	0.3916	5.989	3.127	2.863	4.850
Ag with 20 mM NaBr	0.3895	5.171	2.779	2.393	4.555
Ni	0.3297	2.304	1.128	1.176	1.743
Ni with 20 mM NaBr	0.3800	3.006	1.455	1.611	2.374

The roughness of the Sn coating was found to be 0.4095 µm when the deposition was performed in a bath without NaBr; however, the roughness of the Sn coating increased to 0.6174 µm when the coating was achieved from the same liquid medium in the presence of NaBr. This was consistent with the morphologies of the Sn deposits shown in Fig 4 (a), where NaBr can be adsorbed onto the electrode surface and contribute to the coating, as shown in Fig. 6 (EDX), resulting in an increase in grain size, and thus increased roughness, of the coating. It can be seen in Table 1 that the roughness of the Cu coating decreased to 1.184 µm when NaBr was added to the plating liquid. In the electrodeposition of certain metals, the adsorption of additives onto the electrode surface can lead to a decreased grain size, and thus decreased roughness, of the subsequent coating.[81, 82] Extensive additive adsorption on the surface can block the active sites of the substrate, consequently affecting the nucleation of the metal growth mechanism and hindering metal deposition,[83] as possibly occurred in the deposition of Cu in the presence of NaBr. No significant change in the roughness of the Ag coating was found when NaBr was added, as shown in Table 1. The roughness of the Ni coating was 0.3297 µm, which increased to 0.3800 µm as a result of adding NaBr.

There is a difference in the nucleation mechanism of metals in 1:2 ChCl:EG in the presence of NaBr, though the details of such still remain to be discussed as there have been no previous attempts to determine the nucleation mechanisms of these metals in Ethaline 200-based liquid in the absence and presence of additives. Furthermore, the use of NaBr indicated that the morphology of the above-mentioned metal depositions had been improved significantly and that nucleation had altered on the surface, rather than the observations being the results of bulk effects.

4. CONCLUSIONS

In the electrodeposition of metals from aqueous baths, inorganic and/or organic additives are often used as levellers and brighteners to improve the properties of the resultant coatings, such as their brightness, roughness, thickness and current efficiency. However, few studies to date have considered the influence of additives on the electrodeposition of metals from deep eutectic solvents.

In this work, the results of what we believe to be the first study to date into the effects of sodium bromide on the electrodeposition of Sn, Cu, Ag and Ni from Ethaline 200 have been reported, wherein NaBr was shown to have various effects on the deposition properties of these metals. It was found that NaBr affected Sn, Cu, Ag and Ni deposition, where the morphologies of these metal deposits were significantly altered when NaBr was added to the plating bath. Slight changes in the cyclic voltammograms of Sn, Cu and Ni were observed when using NaBr, whilst a clear reduction in the redox peaks of Ag as a result of adding NaBr to the plating bath was apparent. Surface analysis techniques (SEM and 3D-optical microscopy) showed changes to the morphologies and roughnesses of the metal deposits when NaBr was introduced into the plating bath. 3D microscopy was utilized to investigate the roughness profiles of these surfaces. The roughnesses of the Sn and Ni deposits increased when NaBr was used due to increased rates of deposition, while the surface roughnesses of the Cu and Ag deposits decreased as a result of using NaBr, while others saw a reduced surface roughness. The current efficiencies of the Sn, Cu and Ni deposits increased to 97%, 96% and 98%, respectively, when using NaBr as additives.

References

1. A.P. Abbott, G. Frisch, K.S. Ryder, *Annu. Rev. Mater. Res.*, 43 (2013) 335-358. https://doi.org/10.1146/annurev-matsci-071312-121640
2. M. Schlesinger, M. Paunovic, Modern electroplating, John Wiley & Sons, (2011) University of Windsor, Canada.
3. N. Kanani, Electroplating: basic principles, processes and practice, Elsevier, (2004) Berlin, Germany
4. A. Abbott, G. Frisch, S. Gurman, A. Hillman, J. Hartley, F. Holyoak, K. Ryder, *Chem. Commun.*, 47 (2011) 10031-10033. https://doi.org/10.1039/C1CC13616J
5. A. Collazo, R. Figueroa, X. Nóvoa, C. Pérez, *Surf. Coat. Technol.*, 280 (2015) 8-15. https://doi.org/10.1016/j.surfcoat.2015.08.052
6. Y. Salhi, S. Cherrouf, M. Cherkaoui, K. Abdelouahdi, *Appl. Surf. Sci.,* 367 (2016) 64-69. https://doi.org/10.1016/j.apsusc.2016.01.132
7. K. Wang, H. Pickering, K. Weil, *Electrochim. Acta*, 46 (2001) 3835-3840. https://doi.org/10.1016/S0013-4686(01)00670-3
8. B. Li, K. Guo, C. Liu, *Chin. J. Chem. Eng.,* 23 (2015) 1716-1720. https://doi.org/10.1016/j.cjche.2015.08.001
9. H. Kazimierczak, P. Ozga, A. Jałowiec, R. Kowalik, *Surf. Coat. Technol.*, 240 (2014) 311-319. https://doi.org/10.1016/j.surfcoat.2013.12.046
10. S. Dubent, M. Mertens, M. Saurat, *Mater. Chem. Phys.*, 120 (2010) 371-380. https://doi.org/10.1016/j.matchemphys.2009.11.017
11. N.M. Martyak, R. Seefeldt, *Electrochim. Acta*, 49 (2004) 4303-4311.

https://doi.org/10.1016/j.electacta.2004.03.039

12. W. Zhang, Z. Jiang, G. Li, Q. Jiang, J. Lian, *Surf. Coat. Technol.*, 202 (2008) 2570-2576. https://doi.org/10.1016/j.surfcoat.2007.09.023
13. E. Rudnik, G. Włoch, *Appl. Surf. Sci.*, 265 (2013) 839-849. https://doi.org/10.1016/j.apsusc.2012.11.130
14. N.M. Pereira, S. Salomé, C.M. Pereira, A.F. Silva, *J. Appl. Electrochem.*, 42 (2012) 561-571. https://doi.org/10.1007/s10800-012-0431-3
15. F. Endres, D. MacFarlane and A. Abbott, Electrodeposition from ionic liquids, John Wiley & Sons, (2016) 2 edn.,Weinheim, Germany.
16. Q. Zhang, Q. Wang, S. Zhang, X. Lu, X. Zhang, *ChemPhysChem*, 17 (2016) 335-351. https://doi.org/10.1016/j.electacta.2011.02.095
17. A.P. Abbott, J.C. Barron, G. Frisch, K.S. Ryder, A.F. Silva, *Electrochim. Acta,* 56 (2011) 5272-5279. https://doi.org/10.1016/j.electacta.2011.02.095
18. W. Yang, H. Cang, Y. Tang, J. Wang, Y. Shi, *J. Appl. Electrochem.,* 38 (2008) 537-542. https://doi.org/10.1007/s10800-007-9470-6
19. H.F.N. Al-Esary, PhD thesis, Influence of Additives on Electrodeposition of Metals from Deep Eutectic Solvents, University of Leicester, 2017. http://hdl.handle.net/2381/40869. Accessed 25/05/2019
20. P.C. Andricacos, C. Uzoh, J.O. Dukovic, J. Horkans, H. Deligianni, *IBM J. Res. Developmen.*, 42 (1998) 567-574. https://doi.org/10.1147/rd.425.0567
21. Y.-M. Lin, S.-C. Yen, *Appl. Surf. Sci.*, 178 (2001) 116-126. https://doi.org/10.1016/S0169-4332(01)00306-3
22. K. Kondo, N. Yamakawa, Z. Tanaka, K. Hayashi, *J. Electroanal. Chem*., 559 (2003) 137-142. https://doi.org/10.1016/S0022-0728(03)00110-4
23. A. Milchev, E. Vassileva, V. Kertov, *J. Electroanal. Chem., Interf. Electrochem.,* 107 (1980) 323-336. https://doi.org/10.1016/S0022-0728(80)80204-X
24. M. Esplandiu, H. Hagenström, *Solid State Ionics*, 150 (2002) 39-52. https://doi.org/10.1016/S0167-2738(02)00262-X
25. M. Palomar-Pardavé, M.T. Ramírez, I. González, A. Serruya, B.R. Scharifker, *J. Electrochem.Soc.*, 143 (1996) 1551-1558. https://doi.org/10.1149/1.1836678
26. X.H. Xu, C.L. Hussey, *J. Electrochem. Soc.,* 139 (1992) 1295-1300. https://doi.org/10.1149/1.2069399
27. F. Endres, W. Freyland, *J. Phys. Chem. B*, 102 (1998) 10229-10233. https://doi.org/10.1021/jp9824048
28. A.P. Abbott, K. El Ttaib, G. Frisch, K.S. Ryder, D. Weston, *Phys. Chem. Chem. Phys.*, 14 (2012) 2443-2449. https://doi.org/10.1039/C2CP23712A
29. W. Chen, W. Gao, *Electrochim. Acta*, 55 (2010) 6865-6871. https://doi.org/10.1016/j.electacta.2010.05.079
30. S. Chouchane, A. Levesque, J. Douglade, R. Rehamnia, J.-P. Chopart, *Surf. Coat. Technol*., 201 (2007) 6212-6216. https://doi.org/10.1016/j.surfcoat.2006.11.015
31. M.M. Abou-Krisha, *Appl. Surf. Sci.*, 252 (2005) 1035-1048. https://doi.org/10.1016/j.apsusc.2005.01.161
32. G. Roventi, R. Fratesi, R. Della Guardia, G. Barucca, *J. Appl. Electrochem.*, 30 (2000) 173-179. https://doi.org/10.1023/A:1003820423207
33. Z. Grubač, Ž. Petrović, J. Katić, M. Metikoš-Huković, R. Babić, *J. Electroanal. Chem.*, 645 (2010) 87-93. https://doi.org/10.1016/j.jelechem.2010.04.018
34. F. Chen, Y. Pan, C. Lee, C. Lin, *J. Electrochem. Soc.*, 157 (2010) D154-D158. https://doi.org/10.1149/1.3285108
35. G. Meng, F. Sun, Y. Shaoa, T. Zhang, F. Wang, C. Dong, X. Li, *Electrochim. Acta*, 55 (2010) 5990-5995. https://doi.org/10.1016/j.electacta.2010.05.054

36. E. Rudnik, L. Burzyńska, Ł. Dolasiński, M. Misiak, *Appl. Surf. Sci.*, 256 (2010) 7414-7420. https://doi.org/10.1016/j.apsusc.2010.05.082

37. T. Tsuda, C.L. Hussey, G.R. Stafford, *ECS Trans.*, 3 (2007) 217-231. https://doi.org/10.1149/1.2798664

38. M.R. Ali, A. Nishikata, T. Tsuru, *Journal of Electroanal. Chem.*, 513 (2001) 111-118. https://doi.org/10.1016/S0022-0728(01)00607-6

39. W.R. Pitner, C.L. Hussey, G.R. Stafford, *J. Electrochem. Soc.*, 143 (1996) 130-138. https://doi.org/10.1149/1.1836397

40. S.-P. Gou, I.-W. Sun, *Electrochim. Acta*, 53 (2008) 2538-2544. https://doi.org/10.1016/j.electacta.2007.10.039

41. A.P. Abbott, G. Capper, D.L. Davies, R.K. Rasheed, V. Tambyrajah, *Chem. Commun.,* (2003) 70-71. https://doi.org/10.1039/B210714G

42. E.L. Smith, A.P. Abbott, K.S. Ryder, *Chem. Rev.,* 114 (2014) 11060-11082. https://doi.org/10.1021/cr300162p

43. A.P. Abbott, G. Capper, K.J. McKenzie, K.S. Ryder, *Electrochim. Acta*, 51 (2006) 4420-4425. https://doi.org/10.1016/j.electacta.2005.12.030

44. A.P. Abbott, G. Capper, K.J. McKenzie, A. Glidle, K.S. Ryder, *Phys. Chem. Chem. Phys.,* 8 (2006) 4214-4221. https://doi.org/10.1039/B607763N

45. R. Bernasconi, M. Zebarjadi, L. Magagnin, *J. Electroanal. Chem.*, 758 (2015) 163-169. https://doi.org/10.1016/j.jelechem.2015.10.024

46. P. Sebastian, E. Valles, E. Gomez, *Electrochim. Acta*, 123 (2014) 285-295. https://doi.org/10.1016/j.electacta.2014.01.062

47. A.P. Abbott, G. Capper, D.L. Davies, K.J. McKenzie, S.U. Obi, *J. Chem. Eng. Data*, 51 (2006) 1280-1282. https://doi.org/10.1021/je060038c

48. H.K. Ismail, H.F. Alesary, M.Q. Mohammed, *J. Polym. Res*., 26 (2019) 65. https://doi.org/10.1007/s10965-019-1732-6

49. H.K. Ismail, PhD thesis, Novel Battery Chemistries Using Electrically Conducting Polymers Synthesised from Deep Eutectic Solvents and Aqueous Solutions, University of Leicester, 2017. http://hdl.handle.net/2381/39875. Accessed 25/05/2019

50. A.R. Hillman, K.S. Ryder, H.K. Ismail, A. Unal, A. Voorhaar, *Faraday Discuss.,* 199 (2017) 75-99. http://dx.doi.org/10.1039/C7FD00060J

51. H.F. Alesary, H.K. Ismail, A.F. Khudhair, M.Q. Mohammed, *Orient. J. Chem.*, 34 (2018) 2525. http://dx.doi.org/10.13005/ojc/340539

52. A. Abbott, K. El Ttaib, K.S. Ryder, E. Smith, *Trans. Inst. Met. Finish*., 86 (2008) 234-240. https://doi.org/10.1179/174591908X327581

53. A.P. Abbott, K. El Ttaib, G. Frisch, K.J. McKenzie, K.S. Ryder, *Phys. Chem. Chem. Phys.*, 11 (2009) 4269-4277. https://doi.org/10.1039/B817881J

54. A.P. Abbott, G. Capper, D.L. Davies, R.K. Rasheed, *Chem. - Eur. J.*, 10 (2004) 3769-3774. https://doi.org/10.1002/chem.200400127

55. J.L. Ortiz-Aparicio, Y. Meas, G. Trejo, R. Ortega, T.W. Chapman, E. Chainet, *J. Appl. Electrochem.*, 43 (2013) 289-300. https://doi.org/10.1007/s10800-012-0518-x

56. B. Kavitha, P. Santhosh, M. Renukadevi, A. Kalpana, P. Shakkthivel, T. Vasudevan, *Surf. Coat. Technol*., 201 (2006) 3438-3442. https://doi.org/10.1016/j.surfcoat.2006.07.235

57. K. Boto, *Electrod. Surf. Treatment*, 3 (1975) 77-95. https://doi.org/10.1016/0300-9416(75)90048-6

58. L. Oniciu, L. Mureşan, *J. Appl. Electrochem.*, 21 (1991) 565-574. https://doi.org/10.1007/BF01024843

59. H.F. Alesary, S. Cihangir, A.D. Ballantyne, R.C. Harris, D.P. Weston, A.P. Abbott, K.S. Ryder, *Electrochim. Acta*, 304 (2019) 118-130. https://doi.org/10.1016/j.electacta.2019.02.090

60. N.M. Pereira, C.M. Pereira, A.F. Silva, *ECS Electrochem. Lett.*, 1 (2012) D5-D7. https://doi.org/10.1149/2.003202eel

61. S. Salomé, N.M. Pereira, E.S. Ferreira, C.M. Pereira, A. Silva, *J. Electroanal. Chem.*, 703 (2013) 80-87. https://doi.org/10.1016/j.jelechem.2013.05.007
62. C. Gu, Y. You, X. Wang, J. Tu, *Surf. Coat. Technol.*, 209 (2012) 117-123. https://doi.org/10.1016/j.surfcoat.2012.08.047
63. A.P. Abbott, A. Ballantyne, R.C. Harris, J.A. Juma, K.S. Ryder, G. Forrest, *Electrochim. Acta*, 176 (2015) 718-726. https://doi.org/10.1016/j.electacta.2015.07.051
64. A.P. Abbott, A. Ballantyne, R.C. Harris, J.A. Juma, K.S. Ryder, *Phys. Chem. Chem. Phys.,* 19 (2017) 3219-3231. https://doi.org/10.1039/C6CP08720E
65. A.P. Abbott, G. Capper, K.J. McKenzie, K.S. Ryder, *J. Electroanal. Chem.*, 599 (2007) 288-294. https://doi.org/10.1016/j.jelechem.2006.04.024
66. J. Liu, J. Lei, N. Magtoto, S. Rudenja, M. Garza, J. Kelber, *J. Electroch. Soc.*, 152 (2005) G115-G121. https://doi.org/10.1149/1.1842072
67. S. Miura, H. Honma, *Surf. Coat. Technol.*, 169 (2003) 91-95. https://doi.org/10.1016/S0257-8972(03)00165-8
68. E. Norkus, A. Vaškelis, I. Zakaitė, *Talanta*, 43 (1996) 465-470. https://doi.org/10.1016/0039-9140(95)01775-5
69. F. Hanna, Z.A. Hamid, A.A. Aal, *Mater. Lett.*, 58 (2004) 104-109. https://doi.org/10.1016/S0167-577X(03)00424-5
70. P. Sebastián, E. Vallés, E. Gómez, *Electrochim. Acta*, 112 (2013) 149-158. https://doi.org/10.1016/j.electacta.2013.08.144
71. L. Mirkova, ST. Rashkov, C. Nanev, *Surf. Technol.*, 15 (1985) 181-190. https://doi.org/10.1016/0376-4583(85)90060-3
72. H. Yang, X. Guo, N. Birbilis, G. Wu, W. Ding, *Appl. Surf. Sci.*, 257 (2011) 9094-9102. https://doi.org/10.1016/j.apsusc.2011.05.106
73. J.C. Barron, PhD thesis, The electrochemistry of Zn in deep eutectic solvents, University of Leicester, 2010. http://hdl.handle.net/2381/7916. Accessed 25/05/2019
74. A.P. Abbott, F. Qiu, H.M. Abood, M.R. Ali, K.S. Ryder, *Phys. Chem. Chem. Phys.*, 12 (2010) 1862-1872. https://doi.org/10.1039/B917351J
75. Q. Wang, Q. Zhang, B. Chen, X. Lu, S. Zhang, *J. Electrochem. Soc.*, 162 (2015) D320-D324. https://doi.org/10.1149/2.1001507jes
76. Q. Wang, B. Chen, Q. Zhang, X. Lu, S. Zhang, *ChemElectroChem*, 2 (2015) 1794-1798. https://doi.org/10.1002/celc.201500213
77. J.M. Hartley, C.-M. Ip, G.C. Forrest, K. Singh, S.J. Gurman, K.S. Ryder, A.P. Abbott, G. Frisch, *Inorg. chem.*, 53 (2014) 6280-6288. https://doi.org/10.1021/ic500824r
78. M. Steichen, M. Thomassey, S. Siebentritt, P.J. Dale, *Phys. Chem. Chem. Phys.*, 13 (2011) 4292-4302. https://doi.org/10.1039/C0CP01408G
79. K. Kondo, T. Matsumoto, K. Watanabe, *J. Electrochem. Soc.*, 151 (2004) C250-C255. https://doi.org/10.1149/1.1649235
80. L.N. Schoenberg, *J. Electrochem. Soc.,* 119 (1972) 1491-1493. https://doi.org/10.1149/1.2404029
81. K. Gorbunova, A. Sutiagina, *Electrochim. Acta*, 10 (1965) 367-373. https://doi.org/10.1016/0013-4686(65)87030-X
82. A. Radisic, A.C. West, P.C. Searson, *J. Electrochem. Soc.*, 149 (2002) C94-C99. https://doi.org/10.1149/1.1430719
83. B.G. Pollet, J.-Y. Hihn, T.J. Mason, *Electrochim. Acta*, 53 (2008) 4248-4256. https://doi.org/10.1016/j.electacta.2007.12.059